Journal of Pathology
J Pathol 2005; **207**: 471–482
Published online 13 September 2005 in Wiley InterScience (www.interscience.wiley.com). **DOI:** 10.1002/path.1852

Original Paper

Diagnostic and pathogenetic implications of the expression of hepatic transporters in focal lesions occurring in normal liver

Sara Vander Borght,[1]*# Louis Libbrecht,[1]# Hans Blokzijl,[2] Klaas Nico Faber,[2] Han Moshage,[2] Raymond Aerts,[3] Werner Van Steenbergen,[4] Peter L Jansen,[5] Valeer J Desmet[1] and Tania A Roskams[1]

[1]*Laboratory of Morphology and Molecular Pathology, University of Leuven, Leuven, Belgium*
[2]*Department of Gastroenterology and Hepatology, University Hospital Groningen, Groningen, The Netherlands*
[3]*Department of Abdominal Transplant Surgery, University Hospitals Leuven, Leuven, Belgium*
[4]*Department of Hepatology, University Hospitals Leuven, Leuven, Belgium*
[5]*Department of Gastroenterology and Hepatology, Academic Medical Center, Amsterdam, The Netherlands*

**Correspondence to:*
Sara Vander Borght, Minderbroederstraat 12, 3000 Leuven, Belgium.
E-mail: Sara.vanderborght@uz.kuleuven.ac.be

#Both authors contributed equally.

Received: 5 January 2005
Revised: 12 July 2005
Accepted: 14 July 2005

Abstract

Hepatocellular adenoma and focal nodular hyperplasia (FNH) are benign liver tumours. The differential diagnosis of these lesions and of well- to moderately differentiated hepatocellular carcinomas is often difficult but is very important in view of their different treatment. Although neither type of lesion is connected to the biliary tree, FNHs are cholestatic, whereas this is rarely the case for hepatocellular adenomas. This suggests that hepatocellular uptake and secretion of bile constituents is different in FNHs compared to adenomas. We therefore evaluated the expression and localization of hepatic transporters in hepatocellular adenomas, different types of FNH and well- to moderately differentiated hepatocellular carcinomas in non-cirrhotic liver and compared them with normal liver, using real-time RT-PCR and (semi-)quantitative immunohistochemistry. The parenchymal expression of the uptake transporter OATP2/8 (OATP1B1/3) was minimal or absent in adenoma, while there was strong and diffuse expression in FNH. We observed diffuse parenchymal expression of the basolateral export pump MRP3 in adenomas, while only reactive bile ductules and adjacent cholestatic hepatocytes were MRP3-positive in FNH. The MRP3/OATP2/8 expression pattern of atypical FNHs resembled that of adenomas, suggesting that both types of lesion are related. Most hepatocellular carcinomas showed decreased expression of one or more of the canalicular transporters (MDR1, MDR3, BSEP). The differences in transporter expression profile between FNHs and adenomas are most likely pathogenetically important and may explain why only FNHs are cholestatic. The finding that each type of focal lesion in non-cirrhotic liver has a specific transporter expression pattern may be useful in the establishment of a correct diagnosis by imaging or on needle biopsy.
Copyright © 2005 Pathological Society of Great Britain and Ireland. Published by John Wiley & Sons, Ltd.

Keywords: hepatic transporters; multidrug resistance-associated protein 3; organic anion transporting protein; hepatocellular adenoma; (a)typical focal nodular hyperplasia; (semi-) quantitative immunohistochemistry; real-time RT-PCR; hepatocellular carcinoma

Introduction

Hepatocellular adenoma, focal nodular hyperplasia (FNH) and hepatocellular carcinoma (HCC) are the most frequent and important types of focal primary lesion that occur in an otherwise normal-appearing, non-cirrhotic liver [1]. The differential diagnosis between these three types of lesion is frequently difficult [1–3]. Although nuclear and architectural atypia on a needle biopsy is typical and diagnostic for HCC, these features are less pronounced in well-differentiated cases [4]. It is well known that it is sometimes very difficult or even impossible to distinguish hepatocellular adenoma from FNH correctly based on imaging and histopathological needle biopsy features [2,3]. This issue has become even more complicated due to the existence of lesions that contain features of both typical FNH and hepatocellular adenomas, i.e. the so-called 'telangiectatic' and 'mixed-type' of FNH [5]. Establishing a correct diagnosis before therapeutic interventions are undertaken is very important, since each type of lesion has its own pathobiological characteristics. Due to its malignant nature, a HCC has to be treated by resection. Hepatocellular adenoma is a monoclonal lesion with a considerable risk of malignant transformation or bleeding, so surgical intervention is again the best option [6,7]. Typical FNH is a polyclonal, hyperplastic lesion that arises as a response to vascular alterations, so surgical resection is not mandatory [8–10]. The telangiectatic/mixed FNH

Copyright © 2005 Pathological Society of Great Britain and Ireland. Published by John Wiley & Sons, Ltd.

is an exception to this rule, since recent data indicate that these atypical types of FNH are in fact a variant of hepatocellular adenoma with similar risk of bleeding [11,12], so surgical resection of this lesion seems the best treatment option. Overall, it is clear that ancillary techniques that help in reaching a correct diagnosis of these types of lesion would be helpful.

We have previously described that typical FNHs display cholestatic features, while this is rarely the case for hepatocellular adenomas [13–16]. It has been suggested that the absence of a connection with the biliary tree in FNHs [15,17,18] leads to the accumulation of bile components, causing chronic cholestasis, ductular reaction and a biliary type of fibrosis [13,16]. Remarkably, ductular reaction or other features of cholestasis are not present in hepatocellular adenomas, although this type of lesion also lacks bile ducts and is not connected to the biliary tree [14,15,18]. These findings suggest that there might be important differences between the two types of lesion regarding the expression and function of transporter proteins that regulate hepatocellular uptake and secretion of bile components. Expression of these transporters has been studied in HCC but never specifically for well- to moderately differentiated cases in non-cirrhotic liver, and the results reported in the literature are conflicting [19–21].

Thus, the putative differences between transporter expression in the different types of focal liver lesion might be helpful in establishing a correct diagnosis and might lead to insights into the role of transporters in the pathogenesis of these focal liver lesions. Therefore, the expression of all transporters that are relevant in bile formation (Table 1) were studied in all the types of focal liver lesion described above, using both (semi-)quantitative immunohistochemistry and real-time RT-PCR.

Materials and methods

Liver tissue specimens

Part of the biopsies used in this study were taken from surgically resected hepatocellular adenomas ($n = 8$), typical FNHs ($n = 9$), telangiectatic FNHs ($n = 3$), mixed hyperplastic and adenomatous forms of FNH ($n = 5$), further referred to as 'mixed FNH' and 'well- or moderately differentiated HCCs' in non-cirrhotic liver ($n = 8$). Two of the patients with HCC had taken oral contraceptives for at least 13 years, suggesting the possibility that they originated from hepatocellular adenomas. Between two and nine large specimens were taken from the lesions and embedded in paraffin wax after fixation in 6% formalin. One specimen was snap-frozen in liquid nitrogen-cooled isopentane and stored at −80 °C. In two cases of telangiectatic FNH and all cases of HCC, there was no frozen tissue available.

Patients who were diagnosed as having hepatocellular adenoma ($n = 7$) and FNH ($n = 7$) on the basis of imaging and needle biopsy findings were included. The needle liver biopsies were fixed in B5 solution and embedded in paraffin wax. The diagnosis of adenoma and the different types of FNH was based on the macroscopic and microscopic criteria of Nguyen *et al* [5]. Immunohistochemical staining for cytokeratin 7 (CK7) was performed to help distinguish mixed FNHs from adenomas. The clinical and pathological data of all patients with resected adenoma or (a)typical FNH are summarized in Table 2.

As normal controls, we used seven liver biopsies that showed no morphological abnormalities. Four biopsies were taken from normal-appearing liver at a distance from FNH and fixed in formalin, and three were morphologically normal B5-fixed needle biopsies taken to exclude autoimmune hepatitis, storage disease and congenital hepatic fibrosis. Part of each biopsy was snap-frozen in liquid nitrogen-cooled isopentane. The use of these tissues for the study of hepatic transporter expression was approved by the Local Commission for Medical Ethics and Clinical Studies.

Histochemistry and immunohistochemistry

Immunohistochemistry was mainly performed on frozen sections, unless stated otherwise. Cryostat sections (4 μm thick) were cut, fixed in acetone for 10 min and incubated with the primary antibodies for 30 min at room temperature. The primary antibodies used are listed in Table 1. For all the monoclonal antibodies, including CK7 (clone OV-TL 12/30; Dako, Denmark), the second and third step consisted of peroxidase-labelled rabbit anti-mouse and peroxidase-labelled swine anti-rabbit immunoglobulins (both from Dako) for human liver. For the staining of BSEP, the slides were incubated with a rabbit anti-goat peroxidase-labelled secondary antibody, followed by goat peroxidase anti-peroxidase complex (goat PAP complex; Dako). For the polyclonal antibody against NTCP, the secondary step consisted of peroxidase-labelled swine anti-rabbit IgG followed by peroxidase-labelled rabbit anti-swine IgG (Dako).

For staining of paraffin-embedded material, 5 μm thick sections were dewaxed in xylene followed by rehydration. Endogenous peroxidase activity was blocked using 0.3% H_2O_2 in methanol for 20 min. The paraffin sections were pretreated in citrate buffer (pH 6.0) for 30 min in a hot waterbath at 98.5 °C. The sections were incubated with the primary antibodies for 30 min at room temperature (Table 1) and subsequently incubated for 30 min at room temperature with anti-mouse peroxidase-conjugated Envision antibody (Dako) and in the case of NTCP with anti-rabbit peroxidase conjugated Envision antibody (Dako). For the staining of BSEP, the same incubations as described for frozen sections were applied. Negative controls consisted of omission of the primary antibody.

Table 1. Localization, substrate specificity of hepatobiliary transporters and antibodies used

Transporter	Gene symbol	Localization in normal liver	Uptake/ export	Transported bile components	Antibody				Reference
					Clone	Species	Dilution	Company	
NTCP	*SLC10A1*	Basolateral; hepatocyte	Uptake	Bile salts	K9	RpAb	1:400	(*)	[22]
OATP2 (OATP1B1)#	*SLCO1B1*	Basolateral; hepatocyte	Uptake	Bile salts, organic anions, bilirubin	mESL	MmAb	1:25	Progen Biotechnik	[23]
OATP2/8 (OATP1B1/3)#	*SLCO1B1/3*	Basolateral; hepatocyte	Uptake	Bile salts, organic anions, bilirubin	mMDQ	MmAb	1:25	Progen Biotechnik	[23]
MDR3	*ABCB4*	Apical; hepatocyte	Export	Phosphatidylcholine	P_3II-26	MmAb	1:50	Monosan	[24]
MRP1	*ABCC1*	Basolateral; bile duct	Export	Glutathione, glucuronide conjugates	QCRL3	MmAb	1:50	Santa Cruz	
MRP2	*ABCC2*	Apical; hepatocyte	Export	Glutathione, glucuronide conjugates, bilirubin	M_2I-4	MmAb	1:50	Monosan	[24]
MRP3	*ABCC3*	Basolateral; hepatocyte, bile duct	Export	Bile salts, glucuronide conjugates	M_3II-9	MmAb	1:10	Monosan	[24,25]
					DTX1	MmAb	1:10	Novocastra	
BSEP	*ABCB11*	Apical; hepatocyte	Export	Bile salts		GpAb	1:30	Santa Cruz	
MDR1	*ABCB1*	Apical; hepatocyte, bile duct	Export		JSB-1	MmAb	1:10	Monosan	[26]

BSEP, bile salt export pump; MDR, multidrug resistance protein; MRP, multidrug resistance–associated protein; NTCP, Na^+/taurocholate co-transporting protein; OATP, organic anion transporting protein; MmAb, mouse monoclonal antibody; GpAb, goat polyclonal antibody; RpAb, rabbit polyclonal antibody.

* Kindly provided by Dr Bruno Stieger.

According to the new nomenclature system of Hagenbuch and Meier [27].

On frozen sections, sinusoidal background staining for OATP2, OATP2/8 and NTCP hampered the (semi-)quantitative evaluation, as already reported [23]. Immunohistochemical staining for OATP2 and NTCP did not work on paraffin-embedded material and could therefore only be reliably studied at mRNA level.

MRP3 staining did not work on B5 fixed material, which is the fixative used for needle liver biopsies.

Semi-quantitative and quantitative immunohistochemistry

First, all immunohistochemically stained slides were evaluated for staining patterns and intensities by three observers (SV, LL and TR) using a multi-headed microscope. Quantitative evaluation was performed when there were no clear-cut differences in staining patterns or intensities between adenomas, FNHs and normal liver. For quantitative evaluation, we used a system that measures the mathematical energy (E_M) of the image data file [28]. After acquisition with a 24-bit RGB digital camera of five random fields of each slide at $\times 1000$ magnification, the image file was opened in Adobe Photoshop. The relevant regions of interest, in this case the canalicular or basolateral membranes, were identified in both the stained and the negative control slides using the Magic Wand tool. The region of interest was then used to calculate the E_M using the software program Tiffalyzer. The E_M specifically due to the immunohistochemical reaction product was determined by calculating the absolute value of the difference between the experimental and negative control slide.

RNA isolation and real-time RT-PCR

After sections were cut for immunohistochemistry, the frozen liver biopsies were used to determine the mRNA levels of the transporters. Sufficient material was available for seven adenomas, nine typical FNHs and four normal control livers. Total RNA was extracted from liver tissue using the TRIzol method (Invitrogen Life Technologies, Breda, The Netherlands) according to the manufacturer's instructions.

Reverse transcription was subsequently performed on 2.5 μg total RNA, using random primers in a final volume of 50 μl (Reverse Transcription System, Promega, Madison, WI, USA). cDNA levels of the various transporter genes were measured by real-time PCR, using the ABI PRISM 7700 sequence detector (Applied Biosystems, CA, USA). We used 4 μl 20-fold diluted cDNA in each PCR reaction in a final volume of 20 μl, containing 900 nM sense and anti-sense primers, 200 nM fluorogenic probe, 5 mM $MgCl_2$ and 0.2 mM deoxynucleoside triphosphate mix, Real-Time buffer ($10\times$) and 0.5 U Hot Goldstar DNA-polymerase (Eurogentec, Seraing, Belgium). Sequences of the primers and probes used are listed in Table 3. The PCR programme was 95 °C for 10 min, followed by

Table 2. Clinical features of patients and pathological features of their resected hepatocellular adenoma, focal nodular hyperplasia (FNH), mixed FNH or telangiectatic FNH

Lesion	Gender (males/females)	Age* (years)	Diameter* (cm)	Central scar (yes/no)	Haemorrhage (yes/no)
Adenoma	1/7	33 ± 4	10.0 ± 1.7	0/8	4/4
FNH	2/7	36 ± 3	7.9 ± 1.3	7/2	0/9
Mixed FNH	0/5	28 ± 4	5.6 ± 0.8	1/4	2/3
Telangiectatic FNH	0/3	41 ± 7	4.3 ± 0.8	0/3	2/1

* Values are mean ± SEM.

Table 3. Sequences of PCR primers and probes used for real-time detection PCR analysis

cDNA		Primers
MDR1	Sense	5′-GGC AAA GAA ATA AAG CGA CTG AA-3′
	Antisense	5′-GGC TGT TGT CTC CAT AGG CAA T-3′
	Probe	5′ FAM-CGT GTC CCA GGA GCC CAT CCT GT-TAMRA 3′
MDR3	Sense	5′-TCA ATG GCT TTT AAA GCA ATG CTA-3′
	Antisense	5′-TGC AAT TAA AGC CAA CCT GGT T-3′
	Probe	5′ FAM-CAC AGA TGC TGC CCA AGT CCA AGG A-TAMRA 3′
BSEP	Sense	5′-ACA TGC TTG CGA GGA CCT TTA-3′
	Antisense	5′-GGA GGT TCG TGC ACC AGG TA-3′
	Probe	5′ FAM-CCA TCC GGC AAC GCT CCA AGT CT-TAMRA 3′
MRP1	Sense	5′-CTT CTG GAG GAA TTG GTT GTA TAG AAG-3′
	Antisense	5′-GGT AGA CCC AGA CAA GGA TGT TAG A-3′
	Probe	5′ FAM-TCT TTG AGA TGC TTC TGG CTC CCA TCA C-TAMRA-3′
MRP2	Sense	5′-TGC AGC CTC CAT AAC CAT GAG-3′
	Antisense	5′-CTT CGT CTT CCT TCA GGC TAT TCA-3′
	Probe	5′ FAM-CAG CTT TCG TCG AAC ACT TAG CCG CA-TAMRA 3′
MRP3	Sense	5′-GCC ATC GAC CTG GAG ACT GA-3′
	Antisense	5′-GAC CCT GGT GTA GTC CAT GAT AGT G-3′
	Probe	5′ FAM-CAT CCG CAC CCA GTT TGA TAC CTG CAC-TAMRA 3′
OATP2	Sense	5′-AAG CCA CTT CTG CTT CTG TGT TT-3′
	Antisense	5′-AAT TCT TAG TGA AAG GAC CAG GAA CT-3′
	Probe	5′-FAM-CTC AAA AAT AAC ATC TTA CTG AAT CAA TGC AAT GCT GT-TAMRA 3′
OATP8	Sense	5′-TGA TAT CAC TGG TCC TGG TTC TCA-3′
	Antisense	5′-GCA TGT ATT GTG GCC GTT TG-3′
	Probe	5′-FAM TCC TTG CAC CAT AGG GAT CGT CCT CA-TAMRA 3′
NTCP	Sense	5′-AAC ATG TAA TTT GGA CAT GCA AGA C-3′
	Antisense	5′-TTG TCA GTG AAA GAC CAG GAA CA-3′
	Probe	5′-FAM CTG CTG CCA ACT AAC ATT GCA TTG ATT CAT T-TAMRA 3′
18S	Sense	5′-CGG CTA CCA CAT CCA AGG A-3′
	Antisense	5′-CCA ATT ACA GGG CCT CGA AA-3′
	Probe	5′ FAM-CGC GCA AAT TAC CCA CTC CCG A-TAMRA 3′

40 cycles of 15 s at 95 °C and 1 min at 60 °C. Each sample was analysed in duplicate. 18S expression levels were used as an endogenous control.

Statistics

Statistical analysis was performed using Statview (Abacus Concepts, Berkeley, CA, USA). Data are expressed as mean ± SEM. Comparison of the protein or mRNA expression level between the different groups was performed using analysis of variance (ANOVA) followed by Fisher's PLSD (protected least significant difference) test. Comparison between the expression patterns of relevant transporters and type of lesion was performed using Fisher's exact test. A p value of <0.05 was considered statistically significant.

Results

The results are summarized in Tables 4 and 5.

Expression of transporter proteins in normal liver

We observed strong basolateral staining for OATP2/8 on hepatocytes in the centrolobular area, moderate staining of mid-zonal hepatocytes and absence of OATP2/8 expression in periportal hepatocytes. There was cross-reactivity with the endothelium of the capillaries and arteries, serving as an internal control (Figure 1A). Both observations are in agreement with Cui *et al* [23]. Hepatocytes were completely negative for MRP1 and MRP3, with the exception of a few weakly MRP3-positive perivenular hepatocytes in 2/7 cases. The epithelium lining the bile ducts and ductules showed clear basolateral MRP1 and MRP3 positivity (Figure 1B). These staining patterns are in agreement with our previous findings [29]. As shown previously, normal liver showed strong canalicular expression of MDR1 (Figure 1C), MDR3, MRP2 and BSEP without zonal variation. MDR1 was also expressed by the apical membrane

Table 4. Summary of transporter protein expression profiles. Expression patterns that are helpful for discrimination between the different types of focal lesions are indicated in bold

			FNH		
Transporter	**Normal liver ($n = 7$)**	**Adenoma ($n = 8$)**	**Typical ($n = 9$)**	**Atypical ($n = 8$)**	**HCC ($n = 8$)**
OATP2/8	Hepatocyte expression in centrolobular and midzonal areas	**No or only focal hepatocyte expression**	**Diffuse hepatocyte expression, but negative periseptal hepatocytes**	**No or only focal hepatocyte expression**	No consistent expression pattern
MRP3	Hepatocytes are negative; cholangiocytes are positive	**Diffuse expression by hepatocytes**	**Positive reactive bile ductules and periseptal hepatocytes; no expression in rest of parenchyma**	Hepatocytes are negative; positive reactive bile ductules	No consistent expression pattern
MRP2	Expression in hepatocytes throughout the lobule	Expression in hepatocytes	**Expression in hepatocytes**	Expression in hepatocytes	No consistent expression pattern
MDR1, MDR3, BSEP	Expression in hepatocytes throughout the lobule and MDR1 also in cholangiocytes	Preserved normal expression	**Preserved normal expression**	**Preserved normal expression**	**Minimal or no expression in most cases; preserved expression in a minority**

Table 5. Correlation between expression patterns of relevant transporter proteins and type of lesion

		Benign lesion		**Malignant lesion**	
Expression pattern of transporters		**Typical FNH ($n = 9$)**	**Atypical FNH/ adenoma ($n = 16$)**	**HCC ($n = 8$)**	***p* Value**
OATP2/8	+	9/5*	2/0*	n.a	<0.0001/0.0210*
	− Or focal +	0/2*	14/7*		
MRP3	Diffusely +	0	11	n.a	=0.0010
	Periseptal +	9	5		
MDR1, MDR3 or BSEP	Diffusely +	25		0	<0.0001
	− Or decreased	0		8	

n.a, not applicable — no consistent expression pattern.
* Resected cases/needle biopsies. −, negative; +, positive.

of cholangiocytes that lines bile ducts and ductules [29,30].

Expression of transporter proteins in adenomas

On the OATP2/8-staining, four adenomas were completely negative and four showed a few small groups of positive hepatocytes (Figure 2A). The needle biopsies of all seven adenomas showed an OATP2/8 staining pattern that was identical to that observed in resection specimens. All hepatocytes in all adenomas expressed MRP3 at their basolateral pole, irrespective of their localization within the tumour (Figure 2B). No MRP1 expression was observed, with the exception of one adenoma in which there was diffuse and strong expression of MRP1 on basolateral membranes of hepatocytes. MDR1, MDR3, MRP2 and BSEP were strongly and diffusely expressed at the canalicular pole in all adenomas (Figure 2C), which is identical to the expression in normal liver. Quantitative evaluation was performed to exclude small differences in staining intensities that could be missed by semi-quantitative evaluation. Quantitative evaluation confirmed that the parenchymal expression of the canalicular transporters was not different between normal livers and adenomas ($p \geq 0.0630$).

Expression of transporter proteins in typical FNHs

All FNHs showed strong OATP2/8 basolateral staining of hepatocytes throughout the lesion, except for a few layers of OATP2/8-negative periseptal hepatocytes in continuity with reactive ductules (Figure 3A). These hepatocytes were CK7-immunoreactive, which reflects the accumulation of bile salts and is referred to as 'cholate stasis' (Figure 3B) [31]. The needle biopsies from 5/7 FNHs showed an OATP2/8 staining pattern that was identical to that observed in resection specimens. The needle biopsies from two FNHs were negative for OATP2/8. Remarkably, haematoxylin/eosin-stained sections showed sinusoidal dilatation and congestion within the lesion and both women took oral contraceptives. Together with the negative staining, this suggests that these lesions may have been mixed or telangiectatic FNHs that were not recognized as

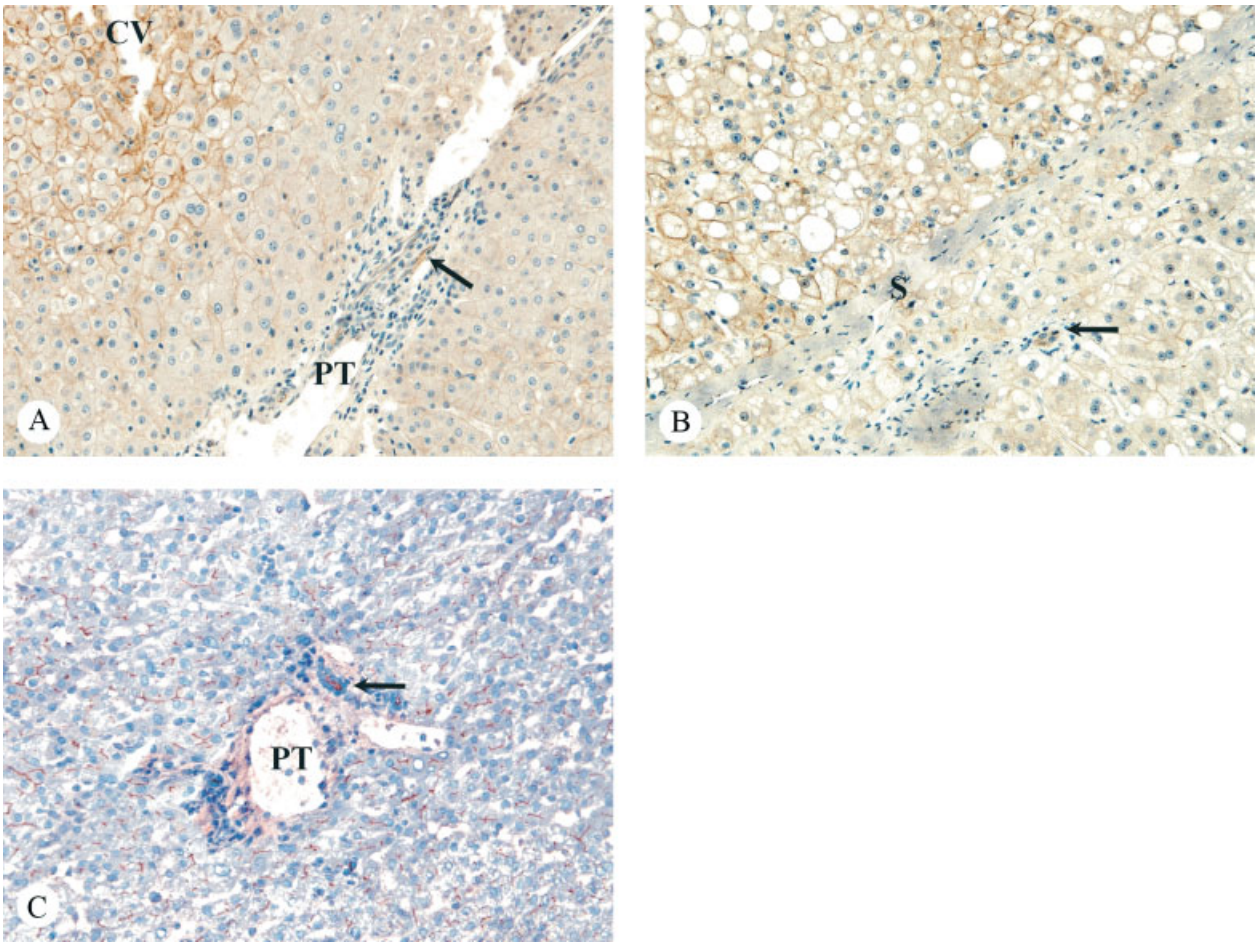

Figure 1. Immunohistochemical staining for OATP2/8 (A), MRP3 (B) and MDR1 (C) in normal liver. (A) There is strong basolateral staining of hepatocytes surrounding the central vein (CV), moderate staining of mid-zonal hepatocytes and absence of OATP2/8 expression in peri-portal hepatocytes. The arterial endothelium in the portal tract (PT) is OATP2/8-positive (arrow). (B) Adenoma (upper left) separated from normal, surrounding parenchyma (lower right) by a thin septum (S). In the surrounding parenchyma, only the bile duct in a portal tract (arrow) is positive. In contrast, hepatocytes in the adenoma are diffusely and strongly positive. (C) Normal liver shows canalicular MDR1 immunoreactivity of the hepatocytes and apical staining of the interlobular bile duct (arrow) in the portal tract (PT). Original magnifications $\times 200$

such on routine diagnostic work-up. Unfortunately, a resection specimen was not available to confirm this.

Reactive bile ductules at the edge of the fibrous septa were strongly immunoreactive for MRP3 (Figure 3C) and MRP1. Hepatocytes were consistently negative for MRP1. The periseptal hepatocytes in continuity with the reactive bile ductules were slightly to moderately positive for MRP3, but there was no MRP3 expression elsewhere in the parenchyma (Figure 3C). The MRP3-positive hepatocytes adjacent to the ductules were also positive for CK7 and correspond to the negative hepatocytes on the OATP2/8 staining. The expression of CK7 and MRP3 by periductular/periseptal hepatocytes is a pattern that is also seen in advanced stages of primary biliary cirrhosis [29,32].

In view of its potential diagnostic value, staining for MRP3 was also performed on paraffin-embedded biopsies from resected adenomas and FNHs, with identical results to those obtained with frozen tissue.

Strong canalicular expression without zonal variation was observed for MDR1, MDR3, MRP2 and BSEP in all FNHs (Figure 3D) and quantitative evaluation confirmed that the expression was not different from adenomas and normal liver ($p \geq 0.0630$).

Expression of transporter proteins in mixed and telangiectatic FNHs

As expected, all staining for MDR1, MDR3, MRP2, BSEP and MRP1 showed an expression pattern identical to that of adenomas and FNHs.

While all the staining for OATP2/8 was performed on paraffin-embedded biopsies, the staining for MRP3 was performed on frozen tissue when available and on paraffin-embedded biopsies in the other cases. Overall, one mixed FNH and one telangiectatic FNH (25% of atypical FNHs) showed a MRP3/OATP2/8 profile that was identical to that of hepatocellular adenomas (Figure 4). In two telangiectatic and three mixed FNHs (63% of atypical FNHs), only one of the two transporters was expressed in the same way as in adenomas. In one mixed FNH (12% of atypical FNHs), the expression profile of hepatocytes at a distance from reactive bile ductules resembled that of typical FNH. Remarkably, the MRP3/OATP2/8 profile of the

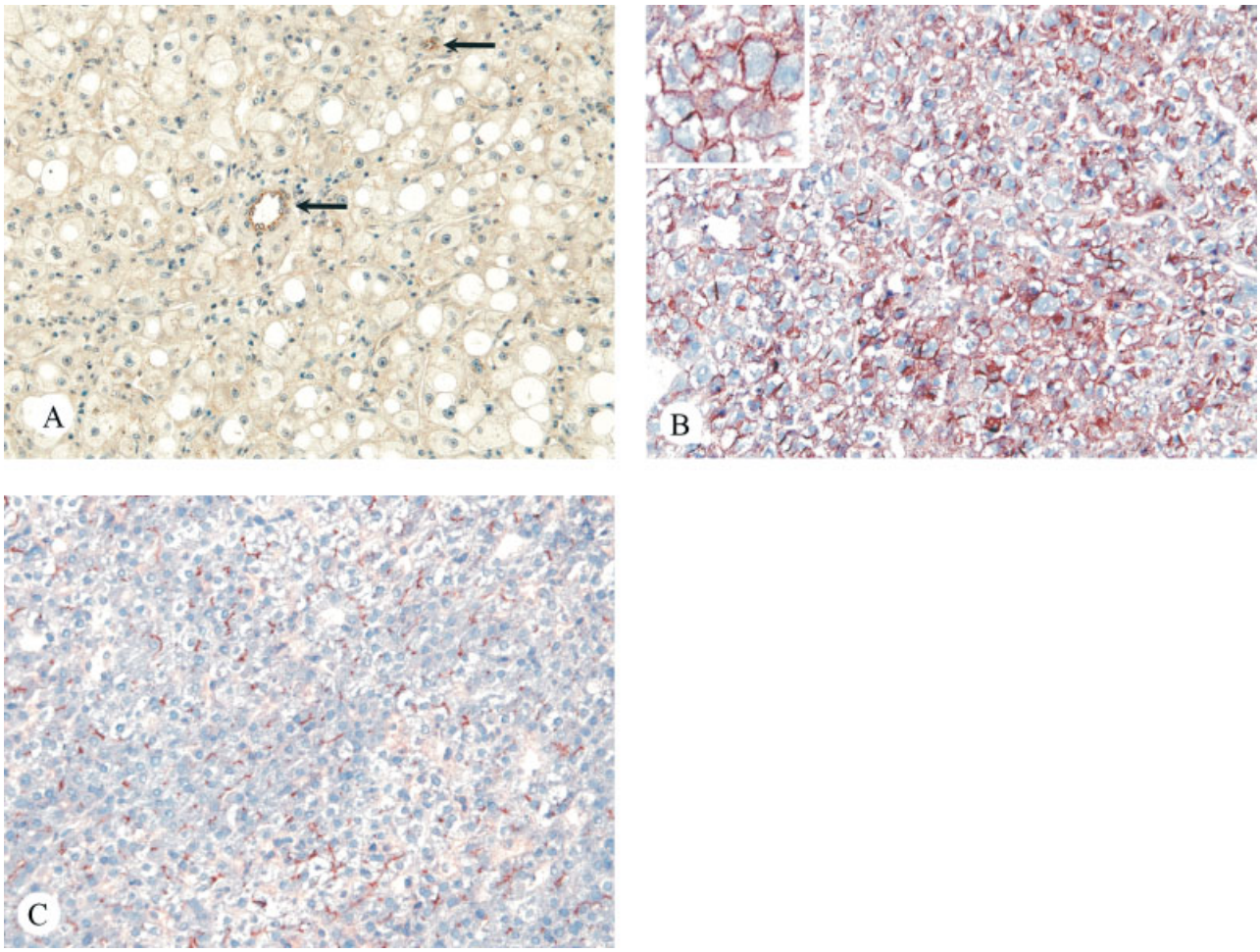

Figure 2. Immunohistochemical staining for OATP2/8 (A), MRP3 (B) and MDR1 (C) in adenoma. (A) All hepatocytes in adenomas are OATP2/8-negative, while arterial endothelium serves as an internal positive control (arrows). (B) Diffuse and strong basolateral expression of MRP3 in adenoma. (C) Canalicular MDR1 staining of the hepatocytes in adenoma. Original magnifications ×200; inset ×400

periseptal hepatocytes was always different from that of their counterparts in typical FNH.

Expression of transporter proteins in well- or moderately differentiated hepatocellular carcinomas in non-cirrhotic liver

The expression patterns and intensities of all the transporters were assessed in eight HCCs in comparison with (surrounding) normal liver by semi-quantitative evaluation. The staining of all transporters in the paraffin-embedded material of normal liver tissue showed the same expression pattern as observed on the corresponding frozen tissue (see above).

Four HCCs showed diffuse basolateral positivity for OATP2/8, which represents an increase since normal peri-portal liver parenchyma is negative. Four HCCs showed no or minimal OATP2/8 expression.

Four HCCs showed basolateral expression of MRP3; four HCCs were completely negative for MRP3, reflecting the absence of parenchymal MRP3 expression in normal liver.

Canalicular MRP2 expression was maintained in five HCCs, while the other three HCCs were negative. Expression of the other canalicular transporters was minimal or absent in most HCCs (Figure 5); clear canalicular expression of MDR1, MDR3 and BSEP was present in two, two and three HCCs, respectively.

Expression of transporter mRNA in adenomas, typical FNHs and normal liver

mRNA expression of the different transporters, normalized for 18S RNA, in the three conditions is summarized in Figure 6, which shows box and whisker plots.

There was a good correlation between protein and mRNA expression of MDR3 and BSEP in control livers, typical FNHs and adenomas. The significantly higher expression of *MDR1* mRNA in FNH compared to adenomas and normal livers correlates nicely with the strong protein expression of MDR1 by reactive ductules that were only present in typical FNHs.

Although there was no difference in mRNA expression of *MRP1*, there was a clear-cut difference in the immunohistochemical staining with strong expression by the reactive bile ductules in typical FNH, while only bile ducts were positive in normal

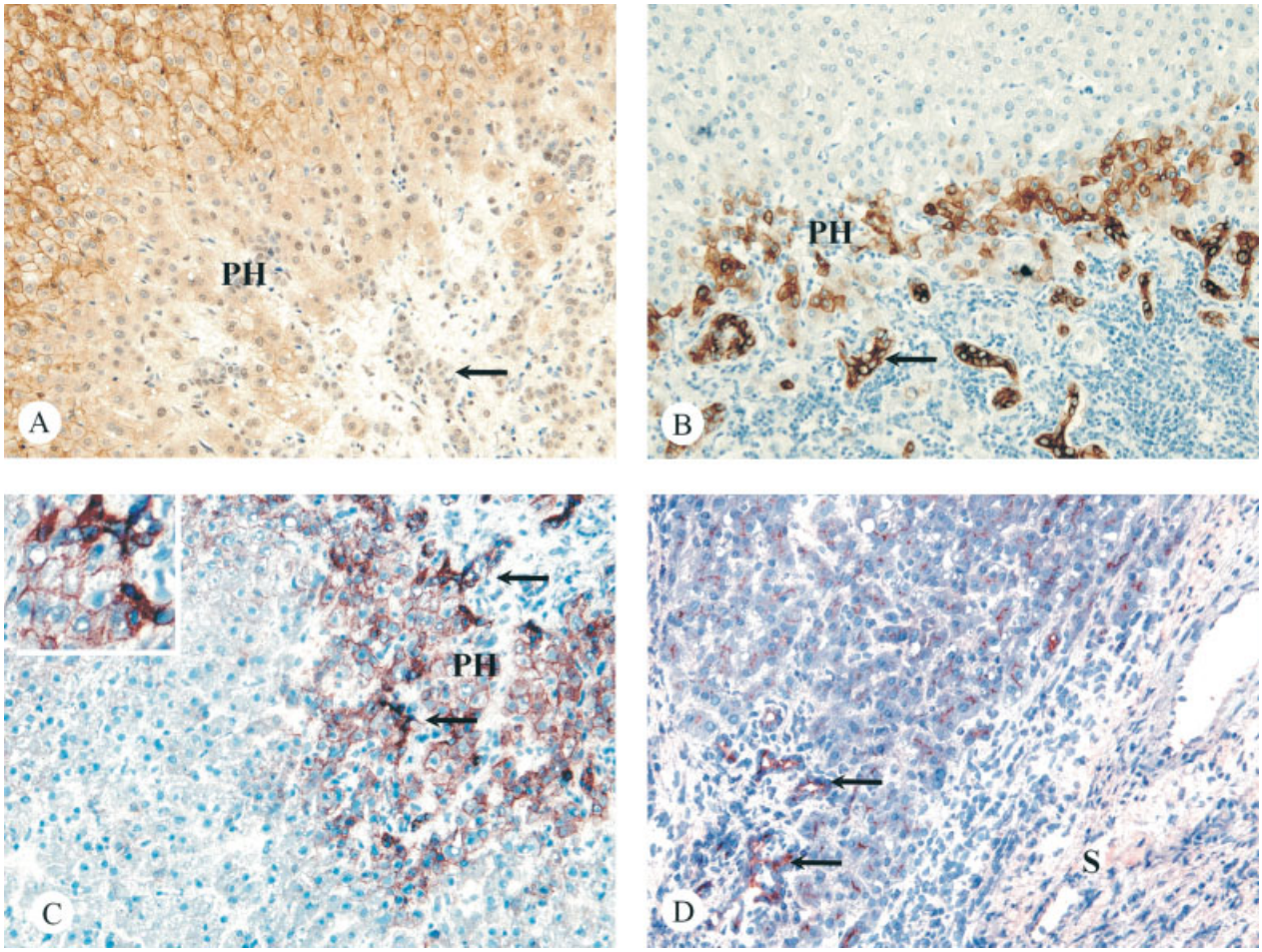

Figure 3. Immunohistochemical staining for OATP2/8 (A), CK7 (B), MRP3 (C) and MDR1 (D) in FNH. (A) Periportal hepatocytes (PH) and reactive bile ductules (arrow) in FNH are negative for OATP2/8 and (B) positive for CK7. In contrast, the remainder of the parenchyma is diffusely and strongly positive for (A) OATP2/8 and negative for (B) CK7. (C) Reactive ductules (arrows) and periseptal hepatocytes (PH) in FNH are strongly and moderately MRP3-positive, respectively, while the remainder of the parenchyma is negative. This expression pattern is very similar to that of CK7 (see Figure 3B). (D) Strong apical MDR1 reactivity of the periseptal (S) reactive bile ductules (arrows) and canalicular staining of the hepatocytes in FNH. Original magnifications ×200; insert ×400

liver and all adenomas except one were completely negative. This suggests that post-transcriptional/post-translational modifications of MRP1 occurring in typical FNH are different from those in adenomas and normal liver.

MRP2 protein expression was identical in all three conditions, while adenomas exhibited lower expression of *MRP2* than typical FNHs at the mRNA level.

While the expression of MRP3 protein was much lower in normal liver than in adenomas and typical FNHs, this was not reflected at the mRNA level. Immunohistochemistry revealed that the difference in MRP3 protein expression between typical FNHs and adenomas was mainly caused by the fact that different compartments express MRP3, i.e. reactive ductules and periseptal hepatocytes in typical FNHs vs the whole parenchyma in adenomas. Such a difference cannot be detected with blotting or PCR using RNA extracted from whole tissue.

The significant and nearly significant differences of *OATP2* and *OATP8* at the mRNA level are in agreement with the findings at the protein level.

Discussion

This is the first study of hepatic transport proteins in focal lesions in non-cirrhotic liver and shows that several transporters are differentially expressed in these lesions. These differences are of potential help in the clinical diagnosis of these lesions and provide insight into the possible role of transporters in the pathogenesis of these lesions.

The finding that the differences in MRP3 and OATP2/8 expression between adenoma (high MRP3, low OATP2/8) and FNH (low MRP3, high OATP2/8) are present diffusely in resection specimens and are reproducible for OATP2/8 in needle biopsies is important: staining of difficult needle biopsies with these antibodies may help in the establishment of a more confident discrimination between hepatocellular adenoma and typical FNH and thus correct treatment.

The expression pattern of most transporters in well- and moderately differentiated HCC in non-cirrhotic liver was variable, although canalicular transporters MDR1, MDR3 and BSEP were mostly absent, which

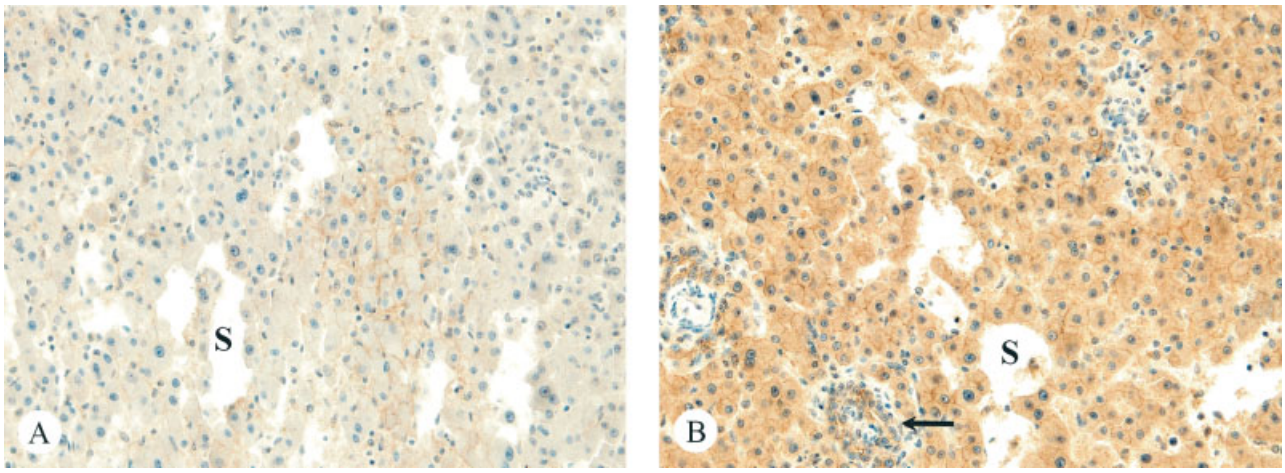

Figure 4. Immunohistochemical staining for OATP2/8 (A) and MRP3 (B) on paraffin sections of a telangiectatic FNH, which is characterized by sinusoidal dilatation (S). (A) OATP2/8 is focally and weakly expressed in the parenchyma and MRP3 (B) is diffusely expressed in the parenchyma and in the reactive bile ductules (arrow). This parenchymal expression pattern is similar to that observed in adenomas (see Figure 2A, B). Original magnifications ×200

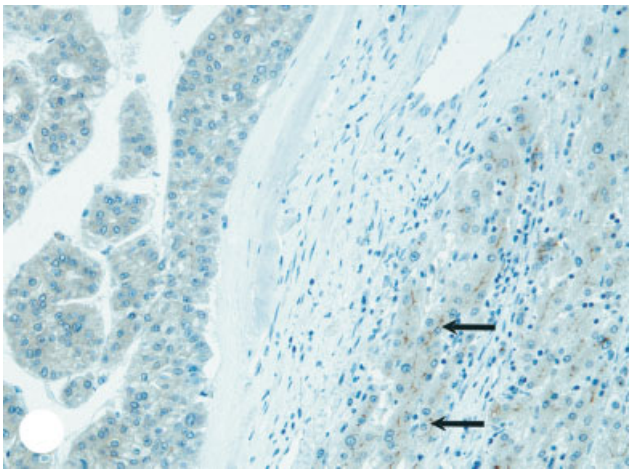

Figure 5. Immunohistochemical staining for MDR1 on a paraffin section of a hepatocellular carcinoma (left) and the surrounding non-cirrhotic liver tissue (right). The surrounding parenchyma shows strong canalicular expression of MDR1 (arrows), while MDR1 expression is absent in the hepatocellular carcinoma. Original magnification ×200

discriminates these HCCs from adenomas and FNHs. Loss of canalicular transporters probably reflects the decrease in differentiation and could be used in diagnostic biopsies as an argument in favour of malignancy.

We found that the MRP3 and OATP2/8 expression pattern in atypical FNHs showed much more resemblance to that of adenomas than to that of typical FNHs. Importantly, the MRP3/OATP2/8 expression profile of periseptal hepatocytes that is characteristic for typical FNHs was never present in atypical FNHs. Our findings confirm recent data that indicate that atypical FNHs are in fact not FNHs but a variant of hepatocellular adenoma that has a similar risk of bleeding and, given its monoclonality, an increased risk of malignant transformation [11,12]. Therefore, it is clinically very important to discriminate atypical FNHs from typical ones and the transporter expression pattern appears to be a helpful tool.

Moreover, our findings may also be of relevance for the emerging field of molecular imaging of focal liver lesions. Several contrast agents that are substrates for specific transporters have been developed in recent years and are being developed. The main problem that hinders the advance and clinical application of this field is the fact that the transporter expression profiles of the different types of focal liver lesions are insufficiently known. Our report of the different expression of MRP3 and OATP2/8 between adenomas, typical FNHs and atypical FNHs should stimulate researchers in the field of molecular imaging to (further) develop contrast agents that are substrates of one of these transporters. Gadolinium B 20 790 might be a good contrast agent for further studies, since it is taken up in *Xenopus laevis* oocytes that express human OATP [33].

Transporter expression profiling is not only helpful in the differential diagnosis of adenoma and FNH, but might also give insight into their pathogenesis. The expression profile of FNHs is very similar to that previously described in advanced PBC [29,32]. Both diseases are characterized by up-regulation of MRP3 expression in the periseptal cholestatic hepatocytes and the adjacent reactive bile ductules. This up-regulation probably represents a pathway to eliminate biliary constituents from these hepatocytes and bile ductular cells towards the sinusoidal blood [29,32,34]. The down-regulation of OATP2/8 in the same hepatocytes can also be seen as an adaptive reaction leading to decreased uptake from the blood. Overall, the expression profile of FNHs is in agreement with the hypothesis that this lesion represents a 'focal biliary fibrosis' that develops secondary to the absence of bile ducts in the lesion [13,16].

A completely different picture was observed in adenomas. These lesions showed diffuse up-regulation of MRP3 and diffuse down-regulation of OATP2/8

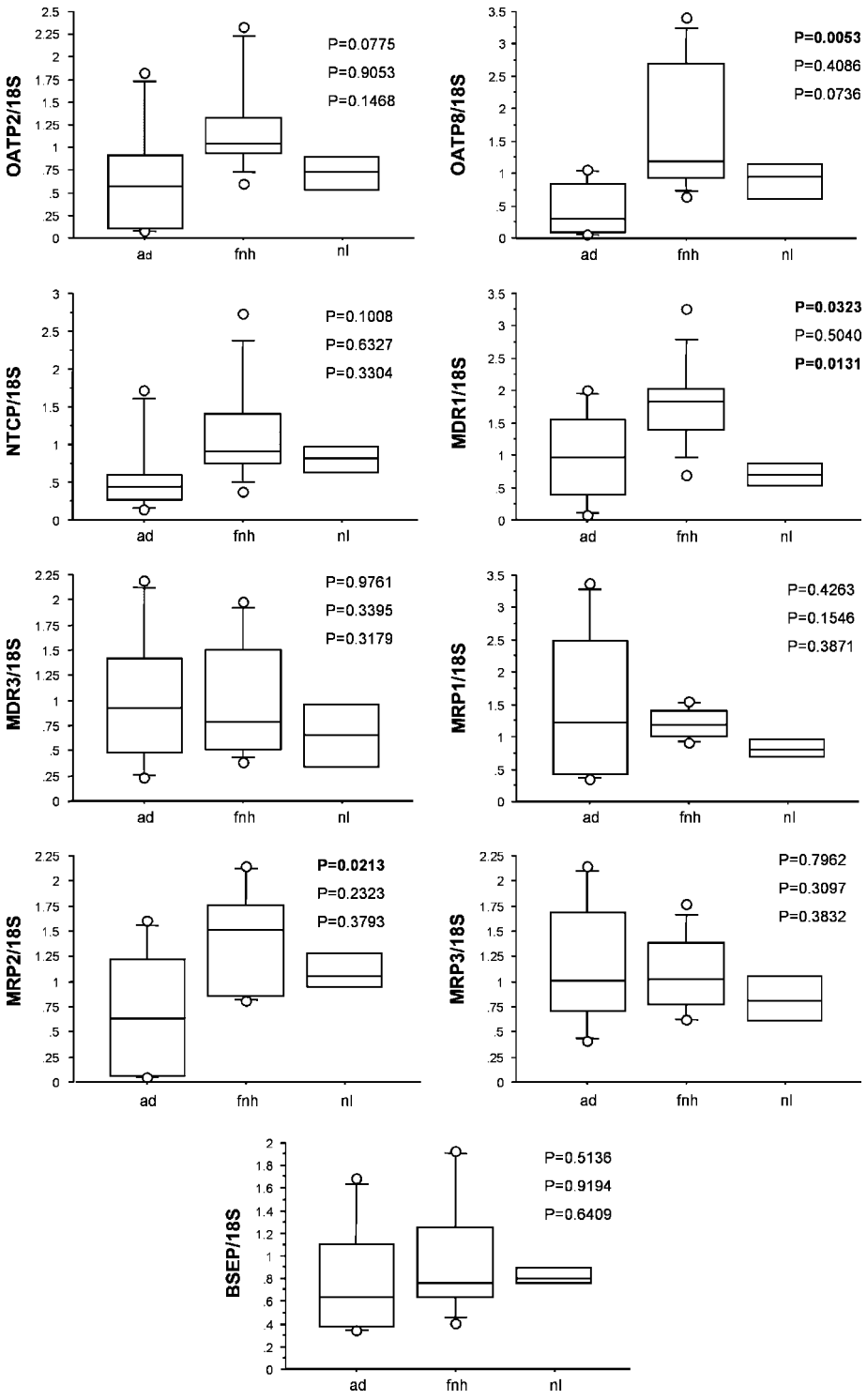

Figure 6. These box and whisker plots represent the median and interquartile ranges of the human hepatobiliary transporter mRNA levels in hepatocellular adenomas (ad), focal nodular hyperplasia (fnh) and normal liver (nl). mRNA levels of the hepatobiliary transporter genes were determined by real-time RT-PCR, as described in Materials and methods. The upper, middle and lower *p* values refer to the comparison between adenoma and FNH, adenoma and normal liver and FNH and normal liver, respectively

in the parenchyma compared to normal liver. These changes are more likely to be primary than a compensatory response to established bile constituent accumulation, since adenomas are much less cholestatic than FNHs [14,15]. According to this view, the changes in transporter expression profiles in adenomas prevent the development of cholestasis and associated damage, and ductular reaction, in a lesion that is devoid of bile ducts. It was recently shown that the majority of hepatocellular adenomas have a biallelic inactivation of the gene transcription factor 1 (*TCF1*), which encodes hepatocyte nuclear factor 1 alpha (HNF1α) [35]. Since this transcription factor activates human OATP2 and OATP8 [36], its inactivation may be (partly) responsible for the downregulation of OATP2/8 observed in the present study

and therefore for the absence of cholestasis and related changes.

Finally, by correlating the mRNA and protein expression of the different transporters in adenomas, typical FNHs and normal liver, we showed that post-transcriptional/post-translational modifications play a role in the expression of MRP1, MRP2 and MRP3 proteins. For example, *MRP2* mRNA was lower in adenoma than FNH, but MRP2 protein expression was not different between the two conditions. This is different from the situation in patients with cholestatic liver disease, where there is an increased MRP2 protein level that is not associated with an increased mRNA expression [32]. In the ligated bile duct rat model of cholestatic liver diseases, *MRP2* mRNA remains unchanged but the protein level decreases [37]. These and our findings underscore the fact that post-transcriptional/post-translational mechanisms are variable and depend on the transporter, the type of disease and the species that is studied. Therefore, the results of studies that investigate transporter expression only at the mRNA level must be interpreted with caution.

In conclusion, we observed diffuse over-expression of MRP3 and down-regulation of OATP2/8 in hepatocellular adenomas, while FNHs had a completely different expression profile that resembled that of chronic biliary diseases. These findings may explain why only FNHs have cholestatic features. In HCCs, canalicular transporters were largely absent, probably as a consequence of dedifferentiation. As such, loss of canalicular transporter expression can be used as an argument in favour of malignancy. The different transporter expression profiles of focal lesions in non-cirrhotic liver may be helpful in establishing a correct diagnosis on a needle biopsy. These profiles also give new insights into the pathogenesis of these lesions and may stimulate the development of molecular imaging contrast agents.

Acknowledgements

Tania Roskams is a Clinical Investigator of the F.W.O.-Vlaanderen. Louis Libbrecht is a 'postdoctoraal onderzoeker' of the F.W.O.-Vlaanderen.

References

1. Hytiroglou P, Theise ND. Differential diagnosis of hepatocellular nodular lesions. *Semin Diagn Pathol* 1998;**15**:285–299.
2. De Carlis L, Pirotta V, Rondinara GF, Sansalone CV, Colella G, Maione G, *et al*. Hepatic adenoma and focal nodular hyperplasia: diagnosis and criteria for treatment. *Liver Transpl Surg* 1997;**3**:160–165.
3. Fabre A, Audet P, Vilgrain V, Nguyen BN, Valla D, Belghiti J, Degott C. Histologic scoring of liver biopsy in focal nodular hyperplasia with atypical presentation. *Hepatology* 2002;**35**:414–420.
4. Kojiro M, Roskams T. Early hepatocellular carcinoma and dysplastic nodules. *Semin Liver Dis* 2005;**25**:133–142.
5. Nguyen BN, Flejou JF, Terris B, Belghiti J, Degott C. Focal nodular hyperplasia of the liver — a comprehensive pathologic study of 305 lesions and recognition of new histologic forms. *Am J Surg Pathol* 1999;**23**:1441–1454.
6. Leese T, Farges O, Bismuth H. Liver-cell adenomas — a 12-year surgical experience from a specialist hepatobiliary unit. *Ann Surg* 1988;**208**:558–564.
7. Zucman-Rossi J. Genetic alterations in hepatocellular adenomas: recent findings and new challenges. *J Hepatol* 2004;**40**:1036–1039.
8. Paradis V, Laurent A, Flejou JF, Vidaud M, Bedossa P. Evidence for the polyclonal nature of focal nodular hyperplasia of the liver by the study of X-chromosome inactivation. *Hepatology* 1997;**26**:891–895.
9. Porayko MK, Choudhary C. Benign neoplasms of the liver. *Curr Treat Options Gastroenterol* 2001;**4**:479–491.
10. Wanless IR, Mawdsley C, Adams R. On the pathogenesis of focal nodular hyperplasia of the liver. *Hepatology* 1985;**5**:1194–1200.
11. Bioulac-Sage P, Rebouissou S, Cunha AS, Jeannot E, Lepreux S, Blanc JF, *et al*. Clinical, morphologic, and molecular features defining so-called telangiectatic focal nodular hyperplasias of the liver. *Gastroenterology* 2005;**128**:1211–1218.
12. Paradis V, Benzekri A, Dargere D, Bieche I, Laurendeau I, Vilgrain V, *et al*. Telangiectatic focal nodular hyperplasia: a variant of hepatocellular adenoma. *Gastroenterology* 2004;**126**:1323–1329.
13. Butron Vila , Haot J, Desmet VJ. Cholestatic features in focal nodular hyperplasia of the liver. *Liver* 1984;**4**:387–395.
14. Libbrecht L, De Vos R, Cassiman D, Desmet V, Aerts R, Roskams T. Hepatic progenitor cells in hepatocellular adenomas. *Am J Surg Pathol* 2001;**25**:1388–1396.
15. Mergo PJ, Ros PR. Benign lesions of the liver. *Radiol Clin North Am* 1998;**36**:319–331.
16. Vaneyken P, Sciot R, Callea F, Desmet VJ. A cytokeratin-immunohistochemical study of focal nodular hyperplasia of the liver — further evidence that ductular metaplasia of hepatocytes contributes to ductular proliferation. *Liver* 1989;**9**:372–377.
17. Ba-Ssalamah A, Schima W, Schmook MT, Linnau KF, Schibany N, Helbich T, *et al*. Atypical focal nodular hyperplasia of the liver: imaging features of nonspecific and liver-specific MR contrast agents. *Am J Roentgenol* 2002;**179**:1447–1456.
18. King LJ, Burkill GJC, Scurr ED, Vlavianos P, Murray-Lyons I, Healy JC. MnDPDP-enhanced magnetic resonance imaging of focal liver lesions. *Clin Radiol* 2002;**57**:1047–1057.
19. Bonin S, Pascolo L, Croce LS, Stanta G, Tiribelli C. Gene expression of ABC proteins in hepatocellular carcinoma, perineoplastic tissue, and liver diseases. *Mol Med* 2002;**8**:316–323.
20. Grude P, Conti F, Mennecier D, Louvel A, Houssin D, Weill B, Calmus Y. *MDR1* gene expression in hepatocellular carcinoma and the peritumoral liver of patients with and without cirrhosis. *Cancer Lett* 2002;**186**:107–13.
21. Zollner G, Wagner M, Fickert P, Silbert D, Fuchsbichler A, Zatloukal K, *et al*. Hepatobiliary transporter expression in human hepatocellular carcinoma. *Liver Int* 2005;**25**:367–379.
22. Kullak Ublick GA, Glasa J, Boker C, Oswald M, Grutzner U, Hagenbuch B, *et al*. Chlorambucil-taurocholate is transported by bile acid carriers expressed in human hepatocellular carcinomas. *Gastroenterology* 1997;**113**:1295–1305.
23. Cui Y, Konig J, Nies AT, Pfannschmidt M, Hergt M, Franke WW, *et al*. Detection of the human organic anion transporters SLC21A6 (OATP2) and SLC21A8 (OATP8) in liver and hepatocellular carcinoma. *Lab Invest* 2003;**83**:527–538.
24. Scheffer GL, Kool M, Heijn M, de Haas M, Pijnenborg ACLM, Wijnholds J, *et al*. Specific detection of multidrug resistance proteins MRP1, MRP2, MRP3, MRP5, and MDR3 P-glycoprotein with a panel of monoclonal antibodies. *Cancer Res* 2000;**60**:5269–5277.
25. Kool M, van der Linden M, de Haas M, Scheffer GL, de Vree JML, Smith AJ, *et al*. MRP3, an organic anion transporter able to transport anti-cancer drugs. *Proc Natl Acad Sci USA* 1999;**96**:6914–6919.
26. Scheper RJ, Bulte JWM, Brakkee JGP, Quak JJ, Vanderschoot E, Balm AJM, *et al*. Monoclonal-antibody Jsb-1 detects a highly conserved epitope on the P-glycoprotein associated with multidrug resistance. *Int J Cancer* 1988;**42**:389–394.

27. Hagenbuch B, Meier PJ. Organic anion transporting polypeptides of the OATP/SLC21 family: phylogenetic classification as OATP/SLCO superfamily, new nomenclature and molecular/functional properties. *Pflugers Arch* 2004;**447**:653–665.
28. Matkowskyj KA, Cox R, Jensen RT, Benya RV. Quantitative immunohistochemistry by measuring cumulative signal strength accurately measures receptor number. *J Histochem Cytochem* 2003;**51**:205–214.
29. Ros JE, Libbrecht L, Geuken M, Jansen PLM, Roskams TAD. High expression of MDR1, MRP1, and MRP3 in the hepatic progenitor cell compartment and hepatocytes in severe human liver disease. *J Pathol* 2003;**200**:553–560.
30. Zollner G, Fickert P, Zenz R, Fuchsbichler A, Stumptner C, Kenner L, *et al*. Hepatobiliary transporter expression in percutaneous liver biopsies of patients with cholestatic liver diseases. *Hepatology* 2001;**33**:633–646.
31. Roskams T. The role of immunohistochemistry in diagnosis. *Clin Liver Dis* 2002;**6**:571–589.
32. Zollner G, Fickert P, Silbert D, Fuchsbichler A, Marschall HU, Zatloukal K, *et al*. Adaptive changes in hepatobiliary transporter expression in primary biliary cirrhosis. *J Hepatol* 2003;**38**:717–727.
33. Pascolo L, Cupelli F, Anelli PL, Lorusso V, Visigalli M, Uggeri F, Tiribelli C. Molecular mechanisms for the hepatic uptake of magnetic resonance imaging contrast agents. *Biochem Biophys Res Commun* 1999;**257**:746–752.
34. Scheffer GL, Kool M, de Haas M, de Vree JML, Pijnenborg ACLM, Bosman DK, *et al*. Tissue distribution and induction of human multidrug resistant protein 3. *Lab Invest* 2002;**82**:193–201.
35. Bluteau O, Jeannot E, Bioulac-Sage P, Marques JM, Blanc JF, Bui H, *et al*. Bi-allelic inactivation of TCF1 in hepatic adenomas. *Nat Genet* 2002;**32**:312–315.
36. Jung D, Hagenbuch B, Gresh L, Pontoglio M, Meier PJ, Kullak-Ublick GA. Characterization of the human OATP-C (SLC21A6) gene promoter and regulation of liver-specific OATP genes by hepatocyte nuclear factor 1 alpha. *J Biol Chem* 2001;**276**:37 206–37 214.
37. Paulusma CC, Kothe MJC, Bakker CTM, Bosma PJ, van Bokhoven I, van Marle J, *et al*. Zonal down-regulation and redistribution of the multidrug resistance protein 2 during bile duct ligation in rat liver. *Hepatology* 2000;**31**:684–693.